

Investigating the viability of PERC solar cells fabricated on Ga- instead of B-doped monocrystalline silicon wafer



Chuanke Chen^a, Hong Yang^a, Jianbo Wang^b, Jun Lv^c, He Wang^{a,*}

^a MOE Key Laboratory for Nonequilibrium Synthesis and Modulation of Condensed Matter, School of Science, Xi'an Jiaotong University, Xi'an, 710049, PR China

^b School of Electronic Science & Engineering, Southeast University, Nanjing, 210096, PR China

^c Electronic Information Engineering College of Sanjiang University, Nanjing, 210012, PR China

ARTICLE INFO

Keywords:

PERC
Ga-doped silicon
Solar cells
LID
Annealing process

ABSTRACT

The viability of commercial Ga-doped silicon PERC solar cell is decided by its efficiency, cost and reliability. In this article, the viability of Ga-doped Cz-Si PERC solar cells has been investigated systematically from an industrial perspective. Firstly, the relationship of wafer resistivity, contact fraction and variation of series resistance for PERC solar cell has been established for increasing the usage rate of Ga-doped crystal. Then, based on the relationship, an average efficiency of 22.21% for the PERC cells with five busbars fabricated from the whole Ga-doped CZ crystal has been achieved. The statistical results of electrical parameters show that the PERC cells fabricated on Ga-doped Cz-Si wafers with a wide resistivity variation (0.5–2.0 Ω·cm) are highly comparable with that of PERC cells made from B-doped Cz-Si wafers with typical resistivity (0.5–1.0 Ω·cm). The obtained results demonstrated that the full range of resistivity values produced from a Ga-doped Cz crystal can be used to fabricate quality, cost-effective PERC solar cells. Meanwhile, a comparative study of initial degradation for optimized Ga-doped PERC solar cells and stabilized B-doped PERC solar cells was carried out in accumulative irradiation of 20 kWh/m² at 50 °C and 80 °C. The results indicate that Ga-doped PERC cells are more stable than stabilized B-doped PERC cells even though at high temperature. The results obtained in this paper demonstrate the viability of Ga- instead of B-doped Cz-Si wafer as substrate to fabricate cost-effective PERC solar cells.

1. Introduction

The conception of passivated emitter and rear cell (PERC) was introduced on laboratory scale by Blakers et al., in 1989 to overcome the efficiency limitation of conventional full aluminum back-surface field (Al-BSF) solar cell [1]. It took more than 25 years from laboratory to industry until cost-effective processes especially in rear passivation and rear contact definition consequences which made benefits in efficiency, economic and throughput available in 2015. The eleventh edition international technology roadmap for photovoltaic (ITRPV) gave a result that rear side passivated solar cell shared more than 70% market in 2020 and this technology will dominate the photovoltaic market over the next 10 years [2]. About 90% of PERC cells were produced on p-type crystalline silicon [2]. The majority of today's p-type silicon wafers use boron as the electrically active dopant since it has the advantage of a high segregation coefficient, which provides minimal resistivity variation in resistivity during crystal growth. However, the minority carrier lifetime in boron-doped silicon wafer is reduced under illumination,

which leads to a degradation in solar cell efficiency [3–6]. The phenomenon is often referred to as light-induced degradation (LID). This degradation mechanism has been investigated and attributed to the formation of boron-oxygen (B–O) related defects [3]. Das and Rohatgi thought that B–O related degradation increase significantly if the surface passivation of cell is improved [7]. Another degradation activated by high-temperature firing process has been observed in multi-crystalline (mc) silicon, float-zone (Fz) and Czochralski (Cz) silicon [8–10]. This degradation is generally highlighted by an elevated temperature of at least 75 °C and called light and elevated temperature induced degradation (LeTID) [11]. Many works gave their results that the efficiency of B-doped PERC solar cells can drop more than 10%_{rel} when exposed to illumination at temperatures above 50 °C [12–14]. It also has been demonstrated that LeTID occurs in Ga-doped solar cell, but the extent of the degradation for Ga-doped solar cell is much reduced compared to B-doped solar cell [15,16]. For commercial B-doped PERC cells, several regeneration processes have been introduced to mitigate the degradation related to B–O defects: annealing the completed solar cells under

* Corresponding author.

E-mail address: pv_group@126.com (H. Wang).

high temperature with high illumination intensity or current injection in the dark [17,18]. Almost all commercial B-doped PERC cell manufacturers apply the latter method [15]. However, these regeneration processes increase the excess costs and process consequences for solar cells fabrication.

The most promising and cost-effective way to against the degradation caused by B–O related defects is that using gallium instead of boron as the dopant during crystal growth, which was suggested in international joint research for light-induced degradation suppression in 1999 [19]. Glunz et al. indicated that Ga-doped Cz-Si as a starting material for photovoltaic application, even if with high interstitial oxygen concentration and low resistivity, it has also showed no degradation, very high lifetime and excellent performance [20–22]. Petter and Grant's work also demonstrated that Ga-doped silicon is significantly less affected by LeTID mechanism [13,15,16]. It has been demonstrated that the potential of Ga-doped Cz-Si for highly efficient solar cell comparable to FZ silicon and magnetic Czochralski (MCz) silicon by a confirmed efficiency of 22.5% [21,23]. Therefore, many researchers thought that Ga-doped Cz wafers are the most promising materials for future advancement toward highly efficient and low-cost solar cells [24–27]. The toughest problem which prevent the commercial application of Ga-doped silicon is the small segregation coefficient (0.008) of gallium in silicon which leads to a great resistivity variation along the Cz ingot [28]. The direct wafer costs of B/Ga-doped Cz wafers are almost the same, because the price of B and Ga dopants are similar, the virgin silicon, crystal growth system used for B/Ga-doped ingot are also the same. The worldwide major Cz wafer supplier LONGi has announced that the price of their Ga-doped Cz-silicon wafer is the same as their B-doped Cz-silicon wafer [29]. However, to maintain the same conversion efficiency of Ga-doped technology identical to B-doped solar cells in market, only small portion of the ingot can be used to fabricate solar cells. This leads to the high cost of Ga-doped solar cells, and makes it uneconomical for commercial application. Some scientists proved that co-doping of gallium with boron in a Cz-Si is an effective way to increase the equilibrium segregation coefficient of Ga in silicon and improve the homogeneity of resistivity over the length of a simply Ga-doped Si crystal [30]. But the minority carrier lifetime of wafers grown by this method would suffer strong degradation from LID [31] and LeTID [32]. Other scientists suggested that continuous Czochralski (CCz) process can be introduced into photovoltaic industry for further improving the uniform of resistivity for longer and larger diameter ingot due to its lower resistivity variation to any dopant than conventional Cz process. Yoon et al. found that the resistivity variation of Ga-doped CCz wafers show better uniformity of dopant distribution compared to conventional Cz wafers [33]. Moreover, compared to recent Cz process, ingot grown by CCz has advantages of lower cost [34].

These technologies push the Ga-doped silicon into photovoltaic industry, but the problem of great resistivity variation along the Ga-doped ingot still remains to be tackled. Many researchers investigated the resistive losses from rear metallization for PERC solar cell. Cox et al. developed an empiric analytical model by separating the total resistance into spreading resistance (R_{sp}), contact resistance (R_c) and residual resistance to evaluate the total resistance of contact alloy for GaAs device [35]. This model was demonstrated to provide a good approximation for R_{sp} in thick PERC cells, but underestimated the R_{sp} in thinner PERC cells [36]. Fischer and Plagwitz et al. presented a model of approximate series resistance (R_s) for PERC solar cell with point and stripe contacts in the rear [37–40]. Gatz et al. optimized specific rear contact resistance (ρ_c) to 40–55 mΩ cm² based on Fischer and Plagwitz model through variating the rear contact fraction (f) of PERC solar cells [41]. However, Müller et al.'s work demonstrated that the series resistance analysis of PERC solar cells according to the method of Gatz shows a high uncertainty and the calculation of R_{sp} according to the model of Plagwitz et al. leads to an underestimation of R_{sp} and an overestimation of ρ_c [42]. Their work also demonstrated that rear contact resistance reduces cell efficiency of PERC solar cells only by about 0.1% absolute if

the metallization fractions higher than 3.5%. Kranz et al. carried out a variation of the f of p-type PERC cell with stripe aluminum rear contacts to determine the $\rho_c < 5 \text{ m}\Omega \text{ cm}^2$ [43]. These models are complicated and inconvenient in practical application. In this paper, we presented a model which can be used to fast determine the best rear contact fraction for PERC solar cell fabrication according to the wafer resistivity. After optimizing laser ablation process according to the relationship during cells fabrication, an average efficiency of 22.21% for the PERC cells with five busbars fabricated from the whole Ga-doped CZ crystal has been achieved. The reliability evaluation results of the Ga-doped PERC cells show that Ga-doped PERC cells are more stable than stabilized B-doped PERC cells. The results obtained in this paper prove that the full range of resistivity values produced from a Ga-doped CZ crystal can be used to fabricate quality solar cells, which indicates that gallium can totally instead of boron as the dopant to fabricate cost-effective PERC solar cells in mass production.

2. Experimental details

In this study, pseudo-square Ga-doped and B-doped (100)-orientation monocrystalline silicon wafers with edge length of 156.75 mm and diagonal length of 210 mm were used. The Ga-doped wafers were from one silicon ingot grown in a CCz system. The resistivities of the Ga-doped wafers used in this work were limited in a range of 0.5–2.0 Ω·cm. The B-doped wafers, which have an area of 156.75 mm × 156.75 mm with about 1 Ω·cm resistivity, were from one silicon ingot grown by the same CCz system. Fig. 1 shows the typical process sequences without unusual processing steps for Ga- and B-doped PERC cells fabrication and degradation in this work. Firstly, Ga-doped wafers underwent a pre-cleaning and texture process which using alkaline (NaOH), additive solution and DI water in a ratio of 7: 2: 300 (by volume). A process time of 7 min at 80 °C was used to make a random pyramid light trapping structure on the surface of the wafer. After that, phosphorus diffusion was carried out to form n-type emitter with sheet resistance (about 120 Ω/sq) by using POCl₃ under nitrogen ambient in low pressure condition. Then, before the etching process, wafers suffered a laser doping scheme to form selective emitter structure to reduce the contact resistance for

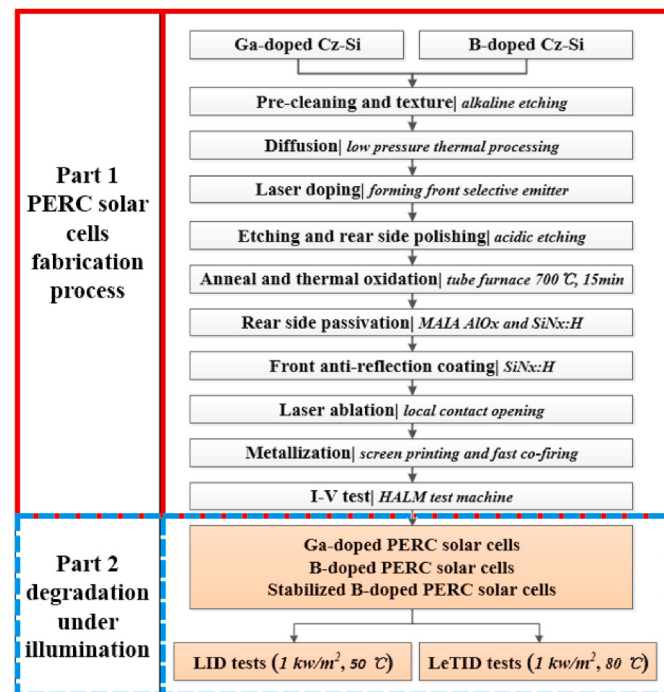


Fig. 1. Process sequences for Ga- and B-doped PERC solar cells fabrication and degradation evaluations at 50 °C and 80 °C.

front metallization. Etching process was performed by using $\text{HNO}_3\text{-HF-H}_2\text{SO}_4$ solution in a ratio of 4: 1: 2 (by volume) to realize edge isolation and rear side polishing. A step of high temperature annealing and thermal oxidation in tube furnace under oxygen (O_2) atmosphere at 700 °C was necessary. And then, the front side and rear side of the wafers were passivated by silicon nitride $\text{SiN}_x\text{:H}$ and $\text{AlO}_x\text{/SiN}_x\text{:H}$ dielectric stacks respectively. The $\text{AlO}_x\text{/SiN}_x\text{:H}$ dielectric stacks were deposited in MAiA tool supplied by Meyer Burger Technology. Then, laser ablation with 532 nm ns laser was carried out on the rear side of the wafer to form a dot matrix geometrical pattern with different opening ratio. The different opening ratio solutions were prepared for the corresponding wafers with different resistivity to optimize the R_s of cells. Finally, H-pattern with five busbars was used for front metallization and the whole rear sides of the cells were covered by aluminum. After the fast-firing process, the current-voltage (I-V) characteristics of the Ga-doped PERC cells were measured by HALM solar cell tester and then they were binned according to their parameters of V_{oc} and I_{sc} . The B-doped PERC cells used in this work underwent the same fabrication process with Ga-doped PERC cells. The structure of these PERC solar cells has been showed in Fig. 2.

Then, the evaluation of efficiencies loss on Ga-doped PERC cells under illumination were carried out. Ga-doped PERC cells, untreated B-doped PERC cells and stabilized B-doped PERC cells were light-soaked under the same condition in laboratory simultaneously. The stabilized and untreated B-doped PERC cells were considered as control groups. The stabilized B-doped PERC cells mean that the cells underwent an annealing process under high current density (8 A) with high temperature (about 160 °C) in the dark ambiance for 45 min. It should be point out that the initial efficiencies of all solar cells in each group are close (see Table 2) in this section. A Xenon lamp with constant light intensity, about 1 sun equivalent illumination was used during the evaluation which were conducted at 50 °C and 80 °C.

3. Results and discussion

3.1. Relationship of series resistance and contact fraction for Ga-doped PERC cell with dashed line pattern

Laser ablation on the rear side of solar cell is an important process to form local contacts through dielectric layers for massive PERC cell fabrication [44–48]. The laser ablation optimization of Ga-doped Cz-Si PERC solar cell need to be more elaborate compared to that of B-doped Cz-Si PERC solar cell since the Ga-doped ingot has a greater resistivity variation. In this section, the relationship of rear contact fraction (f), wafer resistivity (ρ) and variation of series resistance ($R_{s,\text{total}}$) for PERC cell with a dash-contacted back surface was established. This relationship can be used to optimize solar cell's efficiency according to the used wafer resistivity. The f is defined as $f = (n\pi r^2)/(l + g)L_p$, where n is the number of laser spots in a contact point, r is the laser spot radius, l is ablation length, g is ablation gap, and L_p is ablation distance. Fig. 3 shows the rear pattern of PERC cell and details of laser ablation process

in this work. The size, shape and contact fraction (f) of rear contacts could directly affect the spreading resistance (R_{sp}) and contact resistance (R_c) which are significant two parts of series resistance (R_s) of solar cell. Cox et al. [35] defined that

$$R_c = \frac{\rho_c}{S_{\text{contact}}} \quad (1)$$

Where S_{contact} is the area of contact. Fischer [37,38], has proved that when the space between contact points of PERC solar cells is very large, each point can be considered as a separated unit and could not interfere with each other. Then

$$R_{sp} = (l + g)L_p \frac{\rho}{2\pi r} \arctan\left(\frac{2W}{r}\right) \quad (2)$$

Hence, for a single contact point of PERC solar cell with point contact arrays on the rear side, the series resistance brought by the change of wafer resistivity can be written as follows:

$$R_s^* = R_{sp} + R_c = (l + g)L_p \frac{\rho}{2\pi r} \arctan\left(\frac{2W}{r}\right) + \frac{\rho_c}{n\pi r^2} \quad (3)$$

where W is the thickness of wafer, and ρ_c is rear contact resistivity. Fig. 4 shows the equation (3) in comparison with Fischer model which is frequently used in literature for contact resistance calculation [39–42]. Typical wafer thickness, resistivity, laser spot radius and point contact geometries parameters are used for the calculation.

The number of contact points on the rear side of a single cell can be described by $N = S_{\text{wafer}} \times f/(n\pi r^2)$. Assuming each contact point makes the same influence on series resistance, then the variation of series resistance caused by laser ablation for a cell can be rewritten as

$$R_{s,\text{total}} = \frac{R_s^*}{N} = \frac{S_{\text{point}}^2}{2\pi r S_{\text{wafer}}} \arctan\left(\frac{2W}{r}\right) \frac{\rho}{f^2} + \frac{\rho_c}{S_{\text{wafer}} f} \frac{1}{f} \quad (4)$$

where S_{point} and S_{wafer} are the areas of single contact point and wafer respectively. Let

$$k_1 = \frac{S_{\text{point}}^2}{2\pi r S_{\text{wafer}}} \arctan\left(\frac{2W}{r}\right) \quad (5)$$

$$k_2 = \frac{\rho_c}{S_{\text{wafer}}} \quad (6)$$

Hence, equation (4) can be written as

$$R_{s,\text{total}} = k_1 \frac{\rho}{f^2} + k_2 \frac{1}{f} \quad (7)$$

This equation clearly shows the relationship of wafer resistivity, contact fraction and variation of series resistance for a whole cell. It can be used to optimize the laser ablation process fabrication when the cells fabricated on wafers with wide range of resistivity. This equation would greatly be beneficial to achieving the goal of that making the full range of resistivity values produced from a Ga-doped crystal can be used to

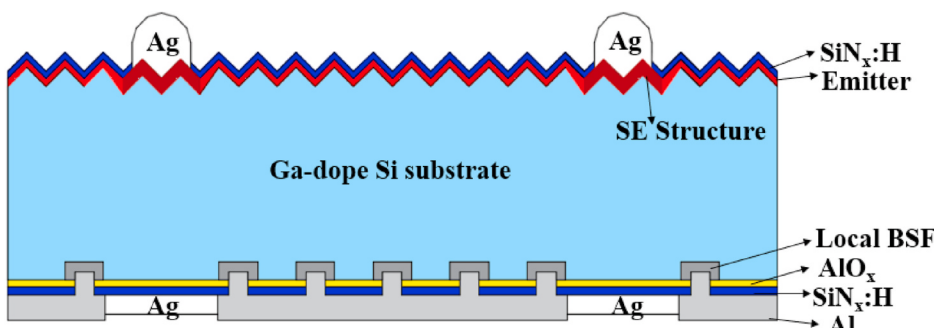


Fig. 2. Schematic diagram of a passivated emitter and rear cell with selective emitter structure (PERC) as fabricated and investigated in this work.

Table 1

Detailed electrical parameters of optimized PERC solar cells fabricated on Ga-doped wafers with different resistivities during laser ablation process optimization.

dopant	group	wafer resistivity ($\Omega \text{ cm}$)	ablation ratio (%)	value	E_{ff} (%)	I_{sc} (A)	V_{oc} (V)	FF (%)	R_s (Ω)	
Ga	A	0.5–1.0	1.03	average	22.21	9.886	0.682	80.47	0.0024	
				best	22.51	9.898	0.686	81.00	0.0023	
	B	1.0–1.5	1.18	average	22.21	9.888	0.682	80.45	0.0024	
				best	22.48	9.901	0.685	81.01	0.0022	
	C	1.5–2.0	1.53	average	22.19	9.890	0.683	80.24	0.0025	
				best	22.48	9.923	0.686	80.62	0.0024	
statistical values for the whole crystal					average	22.21	9.888	0.683	80.39	0.0024

Table 2

Electrical parameters of pre- and post-light soaking evaluation for untreated B-doped PERC solar cells, stabilized B-doped PERC solar cells and Ga-doped PERC solar cells under 5 kWh/m^2 cumulative irradiation at 50 °C and 80 °C.

	dopant	T = 50 °C					T = 80 °C						
		Resistivity ($\Omega \cdot \text{cm}$)	f (%)	E_{ff} (%)	I_{sc} (A)	V_{oc} (V)	FF (%)	E_{ff} (%)	I_{sc} (A)	V_{oc} (V)	FF (%)		
Pre-light soaking	B	0.5–1.0	1.03	group1	22.14	9.870	0.683	80.20	group6	22.16	9.891	0.684	80.07
		0.5–1.0	1.03	group2	21.95	9.873	0.679	79.98	group7	21.93	9.858	0.680	79.96
	Ga	0.5–1.0	1.03	group3	22.16	9.857	0.681	80.60	group8	22.24	9.862	0.684	80.59
		1.0–1.5	1.18	group4	22.13	9.834	0.682	80.65	group9	22.23	9.879	0.684	80.42
Post-light soaking	B	1.5–2.0	1.53	group5	22.14	9.865	0.682	80.45	group10	22.15	9.881	0.683	80.23
		0.5–1.0	1.03	group1	20.93	9.727	0.658	79.95	group6	20.61	9.686	0.654	79.50
	Ga	0.5–1.0	1.03	group2	21.79	9.841	0.678	79.78	group7	21.76	9.860	0.676	79.71
		0.5–1.0	1.03	group3	22.03	9.857	0.680	80.28	group8	22.09	9.873	0.683	80.08
	Ga	1.0–1.5	1.18	group4	22.03	9.851	0.681	80.23	group9	22.09	9.887	0.682	80.05
		1.5–2.0	1.53	group5	22.04	9.838	0.679	80.60	group10	22.02	9.860	0.681	80.08

group1/6: untreated B-doped PERC cells; group2/7: stabilized B-doped PERC cells; group3/8: Ga-doped PERC cells on Cz Si wafers with resistivity ranging from 0.5 to 1.0 $\Omega \cdot \text{cm}$; group4/9: Ga-doped PERC cells on Cz Si wafers with resistivity ranging from 1.0 to 1.5 $\Omega \cdot \text{cm}$; Group5/10: Ga-doped PERC cells on Cz wafers with resistivity ranging from 1.5 to 2.0 $\Omega \cdot \text{cm}$.

fabricate a quality cell. When the wafer resistivity changed, the best contact fraction can be calculated directly through equation (7) by setting $R_{s,\text{total}} = 0$. Fig. 5 shows the relationship between wafer resistivity and the best contact fraction, when $R_{s,\text{total}} = 0$.

For industrial photovoltaic application, low segregation coefficient of gallium in silicon results in a wide distribution of resistivity along the ingot length. Using large resistivity of silicon wafer to fabricate solar cell often leads to high R_s , low FF and low E_{ff} . That's the reason why the resistivity of B-doped Cz-Si ingot widely used in photovoltaic must be controlled at about 1.0 $\Omega \cdot \text{cm}$. However, for Ga-doped ingot, the resistivity of head of the ingot needs to be set higher than B-doped ingot for cost reduction. This situation would cause that one contact fraction value cannot cover the full range of resistivity from a whole Ga-doped ingot and output a large amount of low-quality solar cells.

3.2. Statistical distributions of electrical parameters for Ga- and B-doped PERC solar cells after laser ablation process optimized

Equation (7) has been established to optimize the laser ablation process to mitigate the effects of series resistance from wafer resistivity. In this section, lots of work have been conducted to verify the value of equation (7) for industry application. Three groups of Ga-doped Cz wafers (group A: 0.5–1.0 $\Omega \cdot \text{cm}$, group B: 1.0–1.5 $\Omega \cdot \text{cm}$ and group C: 1.5–2.0 $\Omega \cdot \text{cm}$) from one Ga-doped Cz ingot (see Fig. 6) are used to fabricate PERC cells in pilot line. Based on equation (7), the f of three groups of wafers have been optimized to lower the $R_{s,\text{total}}$ of solar cells which fabricated on the wafers from group B and group C. First, the contact fraction and laser parameters are optimized for group A during the PERC cells fabrication to achieve high efficiencies. Second, the contact fraction of champion efficiency of group A (f_A) will be used to calculate the best contact fractions for group B (f_B) and group C (f_C) by equation (7). Third, the wafers of group B and group C will be put into production line separately to fabricated PERC cell with the f_B and f_C ,

respectively. The detailed electrical parameters of PERC cells fabricated by three groups of Ga-doped wafers are shown in Table 1. The average efficiencies and average series resistances for three groups of wafers are comparable (22.21%, 0.0024 Ω , respectively). The influences of series resistance from wafer resistivity have been reduced by the optimized ablation process. The average efficiency for the whole crystal is 22.21%. The best cell efficiency of 22.51%, with $V_{oc} = 0.686 \text{ V}$ has been achieved in this work.

The statistical distribution of electrical parameters for Ga-doped industrial PERC cells are shown in Fig. 7. For comparison, data of B-doped industrial PERC cells fabricated on B-doped Cz wafers within 0.5–1.0 $\Omega \cdot \text{cm}$ resistivity are also shown in Fig. 7. The B-doped PERC cells underwent the same process with the Ga-doped PERC cells produced by the wafers with 0.5–1.0 $\Omega \cdot \text{cm}$ resistivity. It clearly shows that the average efficiency of Ga-doped PERC cell (22.21%) fabricated from the whole crystal is slightly higher than that of boron doped PERC cells (22.15%). Moreover, the standard deviations (SD) of efficiency distribution for B-/ Ga-doped PERC cells (0.13 and 0.14 respectively) are nearly the same, which means Ga-doped technology is viable as B-doped technology for industrial application. As seen in Fig. 7 (a), (f), (e) and (j), the values of E_{ff} and R_s of Ga-doped PERC cells are comparable to B-doped PERC cells.

3.3. Comparative study of degradation to optimized Ga-doped PERC solar cells and stabilized B-doped PERC solar cells

Researchers have demonstrated that the efficiency of the solar cells, especially the cells with a passivated emitter and rear structure, can significantly degrade under illumination [6,7,49]. Many works also showed reduced susceptibility of LID for Ga-doped wafers [21–27]. Although, for LeTID, Fritz et al. reported that gallium-doped mc-Si showed a slow degradation process under illumination of $0.9 \pm 0.1 \text{ suns}$ at 75 °C [50], there are still few publications to show the degradation of Ga-doped mono-crystalline silicon PERC solar cell under high

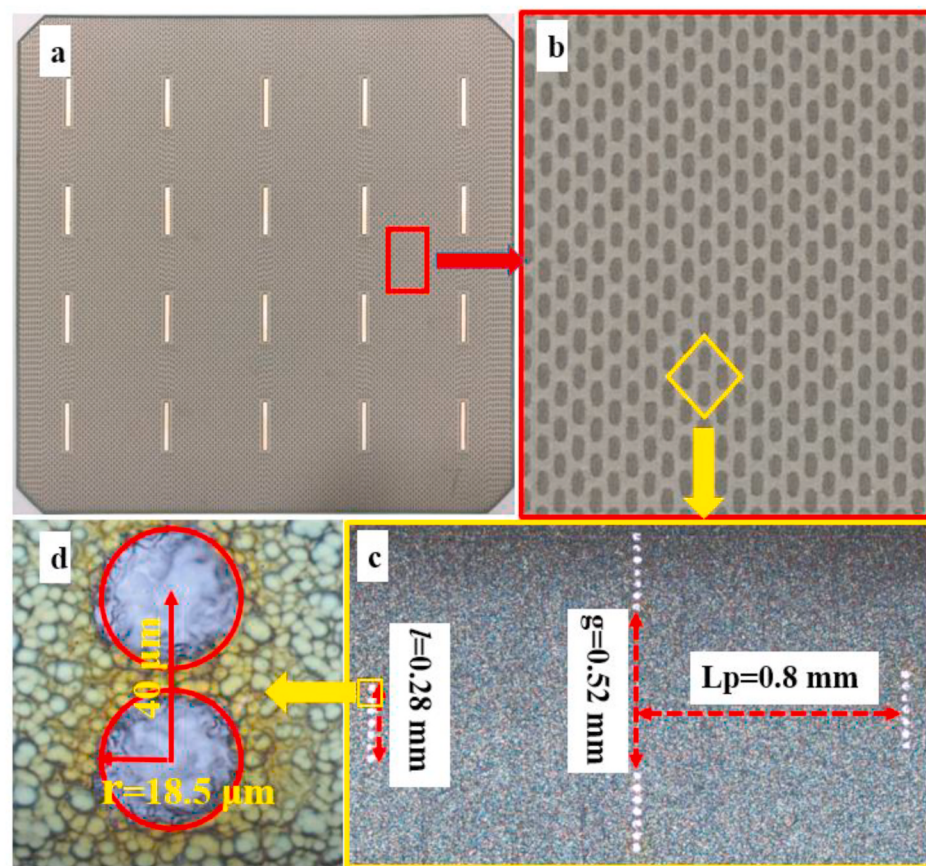


Fig. 3. Rear pattern of PERC cell and details of laser ablation process. (a) Rear pattern of PERC cell; (b) enlarged photograph of rear contact points; (c) ablation image of rear contact points before covered by aluminum paste; (d) laser spot radius.

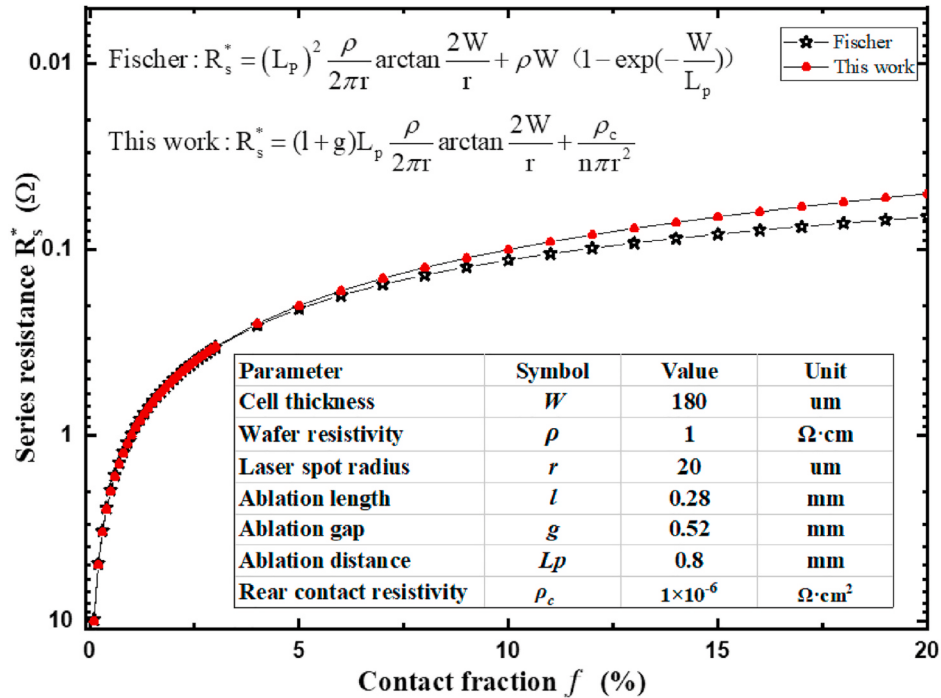


Fig. 4. Comparison between the weighted series resistance, determined by Fischer model and equation (1). Typical wafer thickness, resistivity, laser spot radius and point contact geometries parameters are used for the calculation.

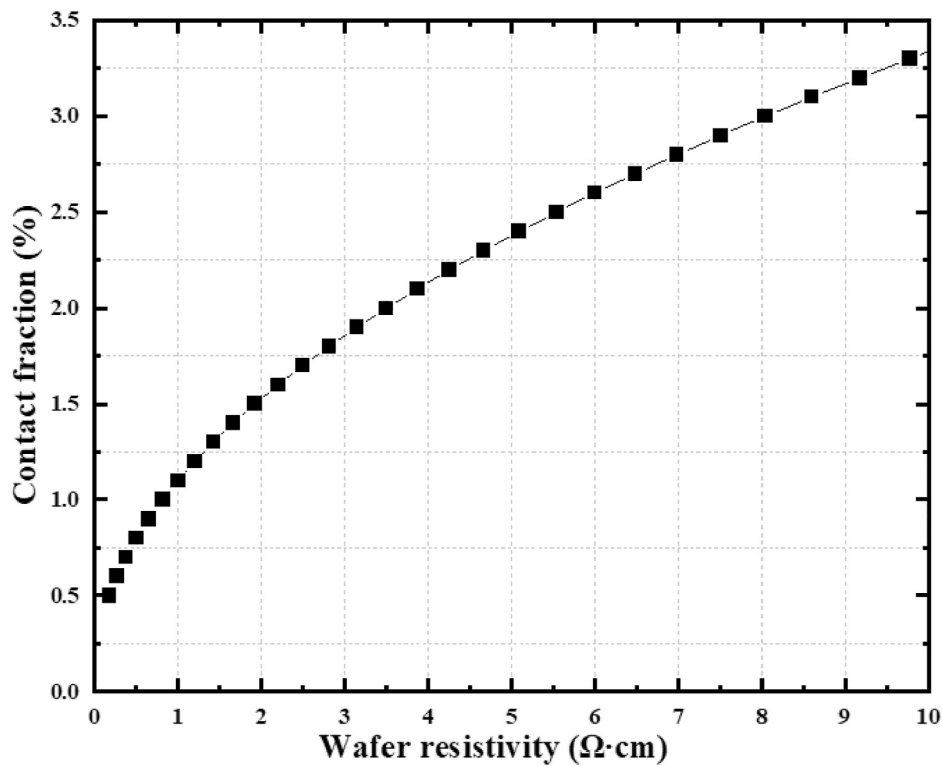


Fig. 5. The relationship between wafer resistivity (ρ) and the best contact fraction (f), when $R_{s,\text{total}} = 0$.

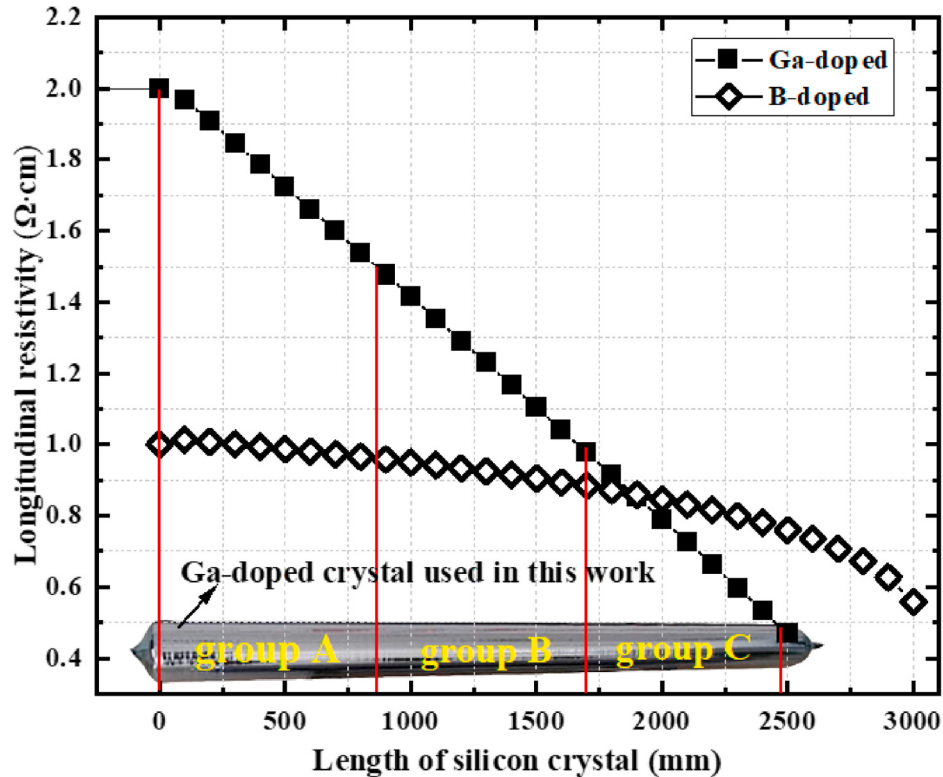


Fig. 6. Theoretical longitudinal resistivity distribution of Cz-Si crystal doped by boron and gallium, respectively.

temperature [6,15,16].

In this section, the degradation of PERC cells made from Ga-doped Cz wafers are investigated under illumination of 1 sun at 50 °C and 80 °C, respectively. The evaluated B-/Ga-doped PERC cells were fabricated in

the same fashion as described above. Details are shown in Table 2. The resistivity of these Ga-doped wafers used for cell fabrication varied from 0.5 to 2.0 $\Omega \cdot \text{cm}$. In addition, the stabilized B-doped PERC cells and untreated B-doped PERC cells are considered as control groups. All cells

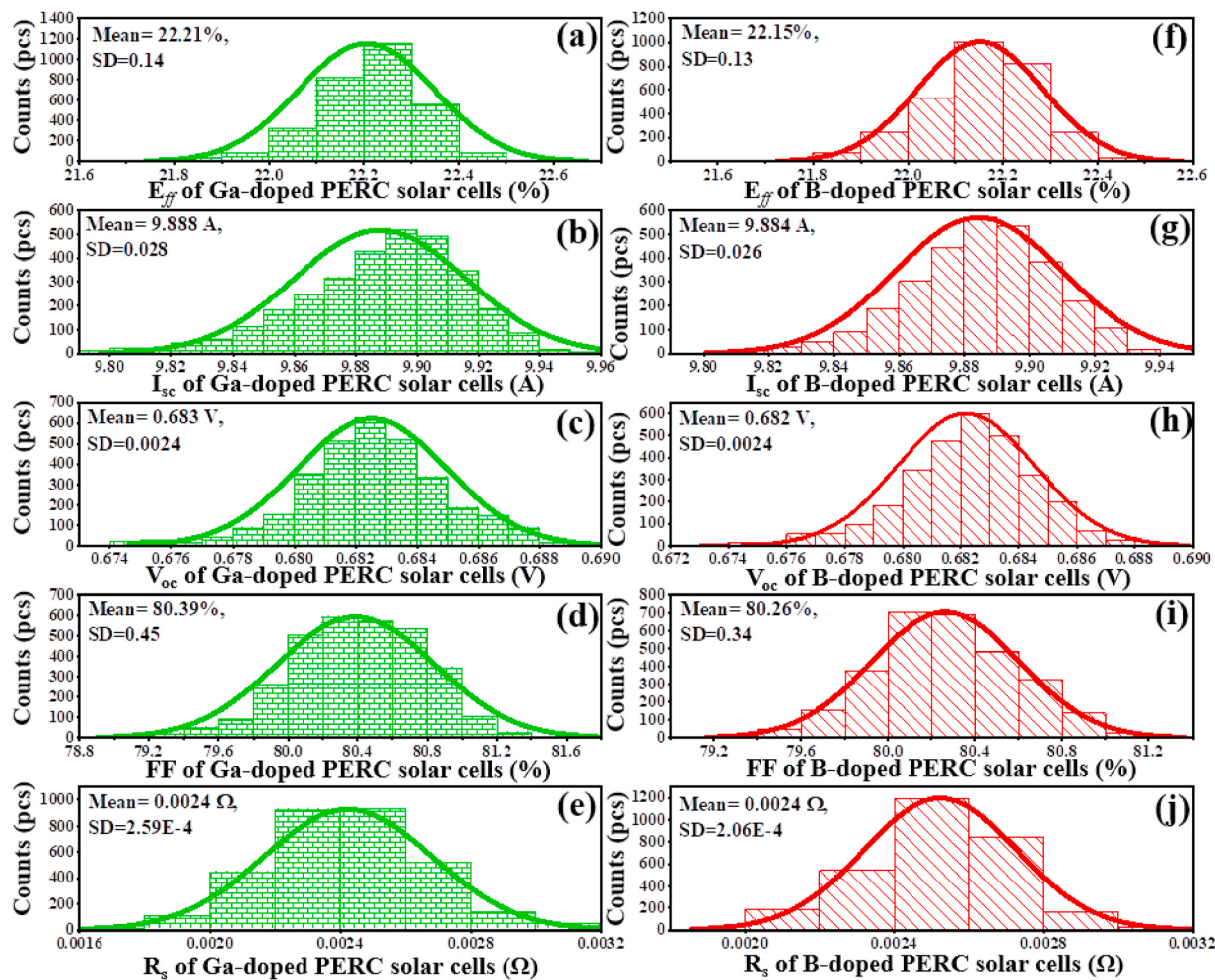


Fig. 7. Statistical distribution of electrical parameters (E_{eff} , I_{sc} , V_{oc} , FF, R_s) for Ga- and B-doped PERC solar cells from pilot line.

in control groups are produced on B-doped Cz-Si with typical resistivity range from 0.5 to 1.0 $\Omega\cdot\text{cm}$. Table 2 shows the pre- and post-light soaking tests results of untreated B-doped PERC cells, stabilized B-doped PERC cells and Ga-doped PERC cells in 5 kWh/m^2 accumulative irradiation when the cells' temperatures are 50 °C and 80 °C, respectively. From Table 2, it can be found that the absolute efficiency loss for untreated B-doped PERC cells at 50 °C and 80 °C are −1.21% and −1.55% respectively, which significantly higher than that of the stabilized B-doped PERC cells (−0.16% and −0.17% respectively) and Ga-doped PERC cells (about −0.1%).

Fig. 8 clearly shows the statistical box charts of relative efficiency loss under light soaking at 50 °C and 80 °C in accumulative irradiation of 20 kWh/m^2 . As seen in Fig. 8, the relative efficiency degradation for untreated B-doped PERC cells (group 1 and group 6) distributes over a large range (over 2%, over 6% at 50 °C and 80 °C, respectively). In addition, from the results of group 6, it can be found that the untreated B-doped PERC cells experienced a re-generation process due to higher temperature, which not happened for other groups of cells. However, all groups of Ga-doped PERC cells (group 3–5 and group 8–10) suffered a slighter degradation (about 0.5% relative) than stabilized B-doped PERC cells (group 2 and group 7). This degradation could be attributed to metal contaminants [51–53]. It is worth mentioning that the Ga-doped PERC cells showed a more serious degradation at 80 °C than at 50 °C. It means that the LeTID also occurs in Ga-doped PERC cells fabricated on mono-Si wafers, but slighter than that of B-doped PERC cells. Additionally, it must be noted that all cells' initial efficiencies for each group stay the same level (see Table 2) before light soaking, but Ga-doped PERC cells show a far more concentrated distribution than that of

B-doped PERC cells after light soaking both at 50 °C and 80 °C. This result indicates that illumination would cause a larger mismatch loss for series connected cells (even though the cells are stabilized) in B-doped PERC solar modules than that of Ga-doped PERC solar modules during field operation.

4. Conclusions

In this study, the relationship among wafer resistivity, contact fraction and variation series resistance of PERC cell has been established. This equation gives a fast, effective way to solve the problems of series resistance brought by the wafer resistivity for Ga-doped PERC cells. The electrical parameters of optimized PERC cells given by equation (7) have proved the value of this method. It can be found that the average efficiencies and average series resistance for Ga-doped PERC cells fabricated on the wafers with different resistivity are nearly the same, which means the negative effects of wafer resistivity on cells have been removed.

The statistical distribution of efficiency and series resistance for B- and Ga-doped PERC cells clearly shows that the optimized Ga-doped PERC cells achieved a higher average efficiency (22.21%) than that of B-doped PERC cells (22.15%) under the same manufacture level. Moreover, the highly closed data of average efficiency and standard deviation for B- and Ga-doped PERC cells verify the potential of Ga-doped Cz-Si for massive industrial application. In addition, the degradation of Ga-doped PERC cells fabricated on the wafers with a wide range of resistivity (0.5–2.0 $\Omega\cdot\text{cm}$) are investigated in accumulative irradiation of 20 kWh/m^2 at 50 °C and 80 °C, respectively. The stabilized

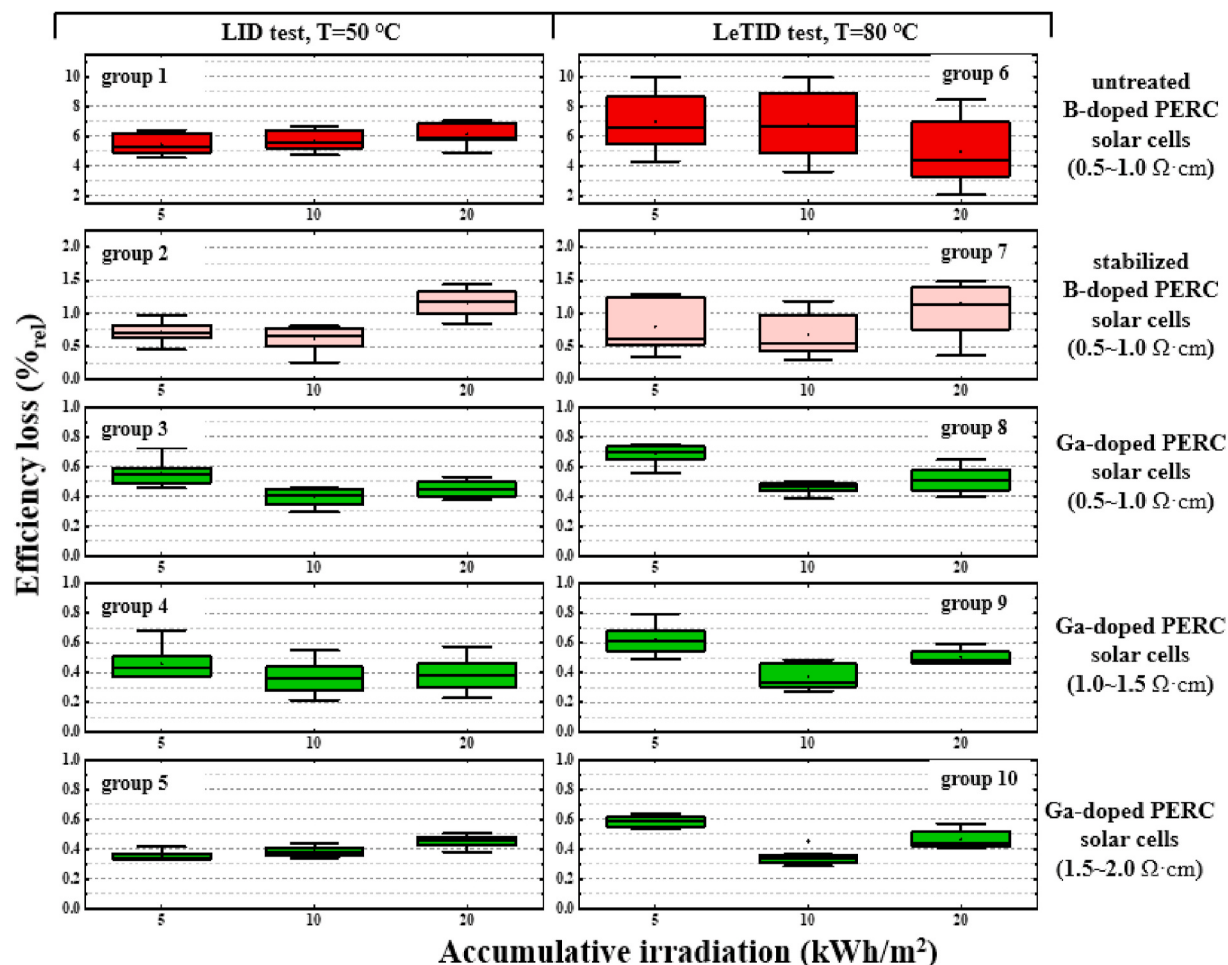


Fig. 8. The statistical box charts of relative efficiency loss against light soaking for untreated B-doped PERC cells, stabilized B-doped PERC cells and Ga-doped PERC cells in accumulative irradiation of 20 kWh/m². group1to group5, at 50 °C; group6 to group10, at 80 °C.

and untreated industrial B-doped PERC cells are considered as contrast groups. The statistical box charts of relative efficiency loss against accumulative irradiation reveal that the performance of Ga-doped PERC cells is much more stable than that of B-doped PERC cells, even though the B-doped PERC cells have been stabilized by an annealing process under high current density with high temperature in the dark. The results presented in this paper prove that Ga-doped silicon wafer can be used as the initial material to fabricate cost-effective PERC solar cells in mass production.

CRediT authorship contribution statement

Chuanke Chen: Conceptualization, Methodology, Investigation, Writing – review & editing. **Hong Yang:** Conceptualization, Methodology, Review. **Jianbo Wang:** Investigation. **Jun Lv:** Investigation. **He Wang:** Writing – review & editing.

Declaration of competing interest

The authors declare that they have no known competing financial interests or personal relationships that could have appeared to influence the work reported in this paper.

Acknowledgements

The authors would like to thank the support of the Natural Science Foundation of China (Grant No. 61376067 and 61274050). This study

was also supported by the National Key R & D Program of China (Grant No. 2018YFB1500700).

References

- [1] A.W. Blakers, A. Wang, A.M. Milne, J. Zhao, M.A. Green, 22.8% efficient silicon solar cell, *Appl. Phys. Lett.* 55 (13) (1989) 1363–1365, <https://doi.org/10.1063/1.101596>.
- [2] <https://itrpv.vdma.org/documents/27094228/29066965/Update0ITRPV02020/2a8588fd-3ac2-d21d-2f83-b896be03e51>.
- [3] J. Schmidt, A.G. Aberle, R. Hezel, Investigation of carrier lifetime instabilities in Cz-grown silicon. Proceedings of the 26th IEEE PVSC, Anaheim, California, USA, 1997, pp. 13–18, <https://doi.org/10.1109/PVSC.1997.653914>.
- [4] K. Bothe, R. Hezel, J. Schmidt, Recombination-enhanced formation of the metastable boron-oxygen complex in crystalline silicon, *Appl. Phys. Lett.* 83 (6) (2003) 1125–1127, <https://doi.org/10.1063/1.1600837>.
- [5] H. Fischer, W. Pschunder, Investigation of photon and thermal induced changes in silicon solar cells, *Proceedings of the 10th IEEE Photovoltaic Specialists Conference*, Palo Alto, CA, USA, 13–15 November 1973, pp. 404–411.
- [6] K. Ramspeck, S. Zimmermann, H. Nagel, A. Metz, Y. Gassenbauer, B. Birkmann, A. Seidl, Light induced degradation of rear passivated mc-Si solar cells, *Proceedings of the 27th European PVSEC*, Frankfurt, Germany, 24–28 September 2012, pp. 861–865, <https://doi.org/10.4229/27thEUPVSEC2012-2D0.3.4>.
- [7] A. Das, A. Rohatgi, The impact of cell design on light induced degradation in p-type silicon solar cells, *PVSC, IEEE ASME Trans. Mechatron.* (2011) 158–164, <https://doi.org/10.1109/PVSC.2011.6185869>.
- [8] M.A. Jensen, A.E. Morishige, J. Hofstetter, D.B. Needleman, T. Buonassisi, Evolution of LeTID defects in p-type multicrystalline silicon during degradation and regeneration, *IEEE J. Photovolt.* 7 (2017) 980–987, <https://doi.org/10.1109/JPHOTOV.2017.2695496>.
- [9] T. Niewelt, M. Selinger, N.E. Grant, W.M. Kwapisil, J.D. Murphy, M.C. Schubert, Light-induced activation and deactivation of bulk defects in boron-doped float-zone silicon, *J. Appl. Phys.* 121 (2017) 185702, <https://doi.org/10.1063/1.4983024>.

- [10] D. Sperber, A. Schwarz, A. Herguth, G. Hahn, Bulk and surface-related degradation in lifetime samples made of Czochralski silicon passivated by plasma-enhanced chemical vapor deposited layer stacks, *Phys. Status Solidi* 215 (2018) 1800741, <https://doi.org/10.1002/pssa.201800741>.
- [11] D. Chen, M. Kim, B.V. Stefani, B.J. Hallam, M.D. Abbott, C.E. Chan, et al., Evidence of an identical firing-activated carrier-induced defect in monocrystalline and multicrystalline silicon, *Sol. Energy Mater. Cells* 172 (2017) 293–300, <https://doi.org/10.1016/j.solmat.2017.08.003>.
- [12] F. Kersten, P. Engelhart, H.C. Ploigt, A. Stekolnikov, T. Lindner, F. Stenzel, M. Bartzsch, A. Szpath, K. Petter, J. Heitmann, J. Müller, Degradation of multicrystalline silicon solar cells and modules after illumination at elevated temperature, *Sol. Energy Mater. Cells* 142 (2015) 83–86, <https://doi.org/10.1016/j.solmat.2015.06.015>.
- [13] K. Petter, K. Hubener, F. Kersten, M. Bartzsch, F. Fertig, B. Kloter, J. Müller, Dependence of LeTID on brick height for different wafer suppliers with several resistivities and dopants, *9th Int. Work. Cryst. Silicon Sol. Cells* (2016) 370–375.
- [14] F. Kersten, F. Fertig, K. Petter, B. Kloter, E. Herzog, M.B. Strobel, et al., System performance loss due to LeTID, *Energy Procedia* 124 (2017) 540–546, <https://doi.org/10.1016/j.egypro.2017.09.260>.
- [15] N.E. Grant, J.R. Scowcroft, A.I. Pointon, M. Al-Amin, P.P. Altermatt, J.D. Murphy, Lifetime instabilities in gallium doped monocrystalline PERC silicon solar cells, *Sol. Energy Mater. Cells* (2020) 206, <https://doi.org/10.1016/j.solmat.2019.110299>.
- [16] N.E. Grant, P.P. Altermatt, T. Niewelt, R. Post, K. Kwapił, M.C. Schubert, J. D. Murphy, Gallium Doped Silicon for High Efficiency Commercial PERC Solar Cells, *Solar RRL*, 2021, <https://doi.org/10.1002/solr.202000754>.
- [17] S. Wilking, C. Beckh, S. Ebert, A. Herguth, G. Hahn, Influence of bound hydrogen states on BO-regeneration kinetics and consequences for high-speed regeneration processes, *Sol. Energy Mater. Cells* 131 (2014) 2–8, <https://doi.org/10.1016/j.solmat.2014.06.027>.
- [18] K. Krauß, A.A. Brand, F. Fertig, S. Rein, J. Nekarda, Fast regeneration processes to avoid light-induced degradation in multicrystalline silicon solar cells, *IEEE J. Photovolt.* 6 (6) (2016) 1427–1431, <https://doi.org/10.1109/JPHOTOV.2016.2598273>.
- [19] T. Saitoh, X. Wang, H. Hashigami, T. Abe, T. Igarashi, S. Glunz, W. Wetting, A. Ebong, B. Damiani, A. Rohatgi, I. Yamasaki, T. Nunoi, H. Sawai, H. Ohtsuka, Y. Yazawa, T. Warabisako, J. Zhao, M. Green, Technical Digest of the 11th International Photovoltaic Science and Engineering Conference, 1999, pp. 553–556.
- [20] S.W. Glunz, S. Rein, W. Warta, J. Knobloch, W. Wetting, Proceedings of the Second World Conference on Photovoltaic Energy Conversion, 1998, pp. 1343–1346. Vienna, Austria.
- [21] S.W. Glunz, S. Rein, J. Knobloch, W. Wetting, T. Abe, Comparison of boron- and gallium-doped p-type Czochralski silicon for photovoltaic application, *Prog. Photovoltaics Res. Appl.* 7 (6) (1999) 463–469, [https://doi.org/10.1002/\(SICI\)1099-159X\(199911/12\)7:6.3.CO;2-8](https://doi.org/10.1002/(SICI)1099-159X(199911/12)7:6.3.CO;2-8).
- [22] S.W. Glunz, S. Rein, J.Y. Lee, W. Warta, Minority carrier lifetime degradation in boron-doped Czochralski silicon, *J. Appl. Phys.* 90 (5) (2001) 2397–2404, <https://doi.org/10.1063/1.1389076>.
- [23] F. Meng, J. Liu, L. Shen, J. Shi, A. Han, L. Zhang, et al., High-quality industrial n-type silicon wafers with an efficiency of over 23% for Si heterojunction solar cells, *Front. Energy Res.* 11 (1) (2017) 78–84, <https://doi.org/10.1007/s11708-016-0435-5>.
- [24] T. Saitoh, X. Wang, H. Hashigami, T. Abe, T. Igarashi, S. Glunz, et al., Suppression of light degradation of carrier lifetimes in low-resistivity CZ-Si solar cells, *Sol. Energy Mater. Cells* 65 (1–4) (2001) 277–285, [https://doi.org/10.1016/S0927-0248\(00\)00103-3](https://doi.org/10.1016/S0927-0248(00)00103-3).
- [25] J. Schmidt, K. Bothe, Structure and transformation of the metastable boron- and oxygen-related defect center in crystalline silicon, *Phys. Rev. B* 69 (2) (2004) 1129–1133, <https://doi.org/10.1103/PhysRevB.69.024107>.
- [26] T. Saitoh, H. Hashigami, X. Wang, T. Abe, T. Igarashi, S. Glunz, S. Rein, W. Wetting, B.M. Damiani, A. Rohatgi, I. Yamasaki, T. Nunoi, H. Sawai, H. Ohtsuka, T. Warabisako, J. Zhao, M. Green, J. Schmidt, A. Cuevas, A. Metz, R. Hezel, Suppression of Light-Induced Degradation of Minority-Carrier Lifetimes in Low-Resistivity CZ-Silicon Wafers and Solar Cells, 16th European PVSEC, 2000, pp. 1206–1211.
- [27] A. Metz, T. Abe, R. Hezel, Gallium-doped Czochralski Grown Silicon: A Novel Promising Material for the PV-Industry, 16th EU PVSEC, 2000, pp. 1189–1194.
- [28] T. Hoshikawa, X. Huang, S. Uda, T. Taishi, Segregation of Ga during growth of Si single crystal, *J. Cryst. Growth* 290 (2) (2006) 338–340, <https://doi.org/10.1016/j.jcrysGro.2006.01.026>.
- [29] https://www.sohu.com/a/396171777_436794.
- [30] R. Gotoh, M. Arivanandhan, K. Fujiwara, S. Uda, Ga segregation during Czochralski-Si crystal growth with Ge co-doping, *J. Cryst. Growth* 312 (20) (2010) 2865–2870, <https://doi.org/10.1016/j.jcrysGro.2010.07.007>.
- [31] M. Arivanandhan, R. Gotoh, K. Fujiwara, S. Uda, Effects of B and Ge co-doping on minority carrier lifetime in Ga-doped Czochralski-silicon, *J. Appl. Phys.* 106 (1) (2009), 013721, <https://doi.org/10.1063/1.3159038>.
- [32] C. Zhou, F. Ji, S. Cheng, J. Zhu, D. Hu, Light and elevated temperature induced degradation in B–Ga co-doped cast mono Si PERC solar cells, *Sol. Energy Mater. Cells* 211 (2020) 110508, <https://doi.org/10.1016/j.solmat.2020.110508>.
- [33] Y. Yoon, Y. Yan, N.P. Ostrom, J. Kim, G. Rozgonyi, Deep level transient spectroscopy and minority carrier lifetime study on Ga-doped continuous Czochralski silicon, *Appl. Phys. Lett.* 101 (22) (2012) 2397, <https://doi.org/10.1063/1.4766337>.
- [34] A.P. Anselmo, V. Prasad, J. Kozioł, et al., Numerical and experimental study of a solid pellet feed continuous Czochralski growth process for silicon single crystals, *J. Cryst. Growth* 131 (s 1–2) (1993) 247–264, [https://doi.org/10.1016/0022-0248\(93\)90420-2](https://doi.org/10.1016/0022-0248(93)90420-2).
- [35] R.H. Cox, H. Strack, Ohmic contacts for GaAs devices, *Solid State Electron.* 10 (12) (1966) 1213–1214, [https://doi.org/10.1016/0038-1101\(67\)90063-9](https://doi.org/10.1016/0038-1101(67)90063-9).
- [36] K.R. Catchpole, A.W. Blakers, Modelling the PERC structure for industrial quality silicon, *Sol. Energy Mater. Sol. Cells* 73 (2) (2002) 189–202, [https://doi.org/10.1016/S0927-0248\(01\)00124-6](https://doi.org/10.1016/S0927-0248(01)00124-6).
- [37] B. Fischer, Metallisation of Silicon Solar Cells, ANU, Canberra, 1994. Diploma thesis.
- [38] B. Fischer, Loss Analysis of Crystalline Silicon Solar Cells Using Photoconductance and Quantum Efficiency Measurements, Doctoral thesis, University Konstanz, Konstanz, 2003.
- [39] H. Plagwitz, M. Schaper, J. Schmidt, B. Terheiden, R. Brendel, Analytical Model for the Optimization of Locally Contacted Solar Cells, Conference Record of the Thirty-First IEEE Photovoltaic Specialists Conference vol. 2005, Lake Buena Vista, FL, USA, 2005, pp. 999–1002, <https://doi.org/10.1109/PVSC.2005.1488301>.
- [40] H. Plagwitz, R. Brendel, Analytical model for the diode saturation current of point-contacted solar cells, *Prog. Photovoltaics Res. Appl.* 14 (1) (2010) 1–12, <https://doi.org/10.1002/pip.637>.
- [41] S. Gatz, T. Dullweber, R. Brendel, Evaluation of series resistance losses in screen-printed solar cells with local rear contacts, *IEEE Journal of Photovoltaics* 1 (1) (2011) 37–42, <https://doi.org/10.1109/JPHOTOV.2011.2163925>.
- [42] M. Müller, F. Lottspeich, Evaluation of determination methods of the Si/Al contact resistance of screen-printed passivated emitter and rear solar cells, *J. Appl. Phys.* 115 (8) (2014) 1363–1365, <https://doi.org/10.1063/1.4867188>.
- [43] C. Kranz, B. Lim, U. Baumann, T. Dullweber, Determination of the contact resistivity of screen-printed Al contacts formed by laser contact opening, *Energy Procedia* 67 (2015) 64–69, <https://doi.org/10.1016/j.egypro.2015.03.288>.
- [44] P. Engelhart, N.P. Harder, T. Horstmann, R. Grischke, R. Brendel, Laser Ablation of Passivating SiN_x Layers for Locally Contacting Emitters of High-Efficiency Solar Cells, Photovoltaic Energy Conversion, IEEE 4th World Conference, IEEE, 2006, <https://doi.org/10.1109/WCPec.2006.279293>.
- [45] S. Hermann, T. Dezhdar, N.P. Harder, R. Brendel, M. Seibt, S. Stroj, Impact of surface topography and laser pulse duration for laser ablation of solar cell front side passivating SiN_x layers, *J. Appl. Phys.* 108 (11) (2010), <https://doi.org/10.1063/1.3493204>, 1363–1005.
- [46] M. Kim, S. Park, D. Kim, Highly efficient PERC cells fabricated using the low cost laser ablation process, *Sol. Energy Mater. Cells* 117 (2013) 126–131, <https://doi.org/10.1016/j.solmat.2013.04.025>.
- [47] P. Hsiao, N. Song, X. Wang, X. Shen, B. Phua, J. Colwell, et al., 266-nm ps laser ablation for copper-plated p-type selective emitter PERC silicon solar cells, *IEEE J. Photovolt.* 8 (2018) 952–959, <https://doi.org/10.1109/JPHOTOV.2018.2834629>.
- [48] H. Felix, H. Christina, S. Sören, M. Agnes, R. Michael, K. Jan, B. Rolf, P. Robby, Laser contact openings for local poly-Si-metal contacts enabling 26.1%-efficient POLO-IBC solar cells, *Sol. Energy Mater. Cells* 186 (2018) 184–193, <https://doi.org/10.1016/j.solmat.2018.06.020>.
- [49] F. Fertig, K. Krauß, S. Rein, Light-induced degradation of PECVD aluminium oxide passivated silicon solar cells, *Phys. Status Solidi Rapid Res. Lett.* 9 (1) (2015) 41–46, <https://doi.org/10.1002/pssr.201409424>.
- [50] J.M. Fritz, A. Zuschlag, D. Skorka, A. Schmid, G. Hahn, Temperature dependent degradation and regeneration of differently doped mc-Si materials, *Energy Procedia* 124 (2017) 718–725, <https://doi.org/10.1016/j.egypro.2017.09.085>.
- [51] J. Lindroos, M. Yli-Koski, A. Haarahiltunen, M.C. Schubert, H. Savin, Light-induced degradation in copper-contaminated gallium-doped silicon, *Phys. Status Solidi Rapid Res. Lett.* 7 (4) (2013) 262–264, <https://doi.org/10.1002/pssr.201307011>.
- [52] T.U. Naerland, S. Bernardini, H. Haug, S. Grini, L. Vines, N.G. Stoddard, et al., On the recombination centers of iron-gallium pairs in Ga-doped silicon, *J. Appl. Phys.* 122 (8) (2017), 085703, <https://doi.org/10.1063/1.5000358>.
- [53] P. Regina, N. Tim, S. Jonas, S. Florian, C.S. Martin, Imaging interstitial iron concentrations in gallium-doped silicon wafers, *Phys. Status Solidi Rapid Res. Lett.* 216 (10) (2019) 1800655.1–181800655.7, <https://doi.org/10.1002/pssa.201800655>. CRediT authorship contribution statement.